Supplemental information for

Water's variable role in protein stability uncovered by liquid-observed vapor exchange NMR.

Candice J. Crilly,[†] Jonathan E. Eicher,[†] Owen Warmuth,[†] Joanna M. Atkin,[†] and Gary J. Pielak*[,†,‡,§,∥]

[†]Department of Chemistry, University of North Carolina at Chapel Hill (UNC-CH), Chapel Hill, North Carolina 27599-3290, United States; [‡]Department of Biochemistry & Biophysics, UNC-CH, Chapel Hill, North Carolina 27599, United States; [§]Lineberger Cancer Center, UNC-CH, Chapel Hill, North Carolina 27599, United States; [∥]Integrative Program for Biological and Genome Sciences, UNC-CH, Chapel Hill, North Carolina 27599, United States

Supplementary text

Materials

Ampicillin, kanamycin sulfate (Sigma Aldrich), trisodium citrate (Agros Organics), citric acid monohydrate and HEPES (Thermo Fisher) were used without further purification. H_2O with a resistivity >17 MΩ cm^{-1} was used to prepare buffers. pH values are direct readings, uncorrected for the deuterium isotope effect.[1] For LOVE NMR experiments, a constant relative humidity of 75 ±5% (measured with a Fisherbrand TraceableGO™ Bluetooth datalogging digital hygrometer) was created as described.[2]

Methods

Protein expression and purification

pET11a plasmids (Novagen) containing the genes for the T2Q and T2Q, I6L variants of the immunoglobulin G binding domain of streptococcal G (WT GB1 and I6L GB1, respectively) were obtained as described.[3] The T2Q mutation prevents N-terminal deamidation.[4] The pET28a plasmid (Novagen) containing the gene for truncated wild-type barley chymotrypsin inhibitor 2 (WT CI2), was provided by Dr. Andrew Lee's laboratory at UNC-Chapel Hill. The first 19 residues of full length CI2 were not included in the construct because they are disordered, and therefore exchange too quickly for observation by NMR. Residue 20 of full-length CI2 is referred to as Residue 1. To create the I20V variant (I20L CI2), site-directed mutagenesis was performed using the following primers (mutated codon in bold).

Forward: 5' A GAA GCG AAA AAA GTG **GTG** CTG CAG GAT AAA C 3'

Reverse: 5' C CGG TTT ATC CTG CAG **CAC** CAC TTT TTT C 3'.

^{15}N-enriched WT GB1, I6L GB1, WT CI2, and I20V CI2 were expressed in Agilent BL21 Gold (DE3) *E. coli* in minimal media and purified as described,[3, 5] with the following modifications for GB1 I6L: Minimal media was supplemented with 2 g/L glycerol, and expression was carried out for ~16 h at 18 °C.

The concentration of purified proteins was determined from the absorbance at 280 nm (A_{280}) (Nanodrop One, Thermo Fisher) using an extinction coefficient of 9530 M^{-1} cm^{-1} for GB1 variants and 7040 M^{-1} cm^{-1} for CI2 variants.[6] Purity was confirmed by Q-TOF mass spectrometry (ThermoScientific, Q Exactive HF-X) in the UNC Mass Spectrometry Chemical Research and Teaching Core Laboratory. Purified protein was exchanged into

H_2O by dialysis (ThermoScientific Snakeskin™ dialysis tubing, 3500 Da molecular weight cutoff), and divided into aliquots such that resuspension in 650 µL gives a protein concentration of 500 µM. Aliquots were flash frozen, lyophilized, and stored at -20 °C.

NMR

Unless noted, experiments were performed in triplicate on Bruker Avance III HD spectrometers with cryogenic QCI probes at ^{1}H Larmor frequencies of 600 MHz for LOVE experiments and 850 MHz for solution amide-proton exchange experiments. For LOVE NMR experiments, sensitivity-enhanced ^{15}N-^{1}H heteronuclear single-quantum coherence (HSQC) spectra were acquired in ~10 min (128 increments in the ^{15}N dimension, 4 scans per increment) with sweep widths of 3041 Hz in the ^{15}N dimension and 8418 Hz in the ^{1}H dimension. For solution exchange experiments, ^{15}N-^{1}H HSQC spectra were acquired in ~10 min (128 increments in the ^{15}N dimension, 4 scans per increment) with sweep widths of 4308 Hz in the ^{15}N dimension and 11904 Hz in the ^{1}H dimension. Spectra were processed with NMRPipe.[7] Cross peaks were integrated using NMRViewJ.[8]

Backbone resonances of WT GB1, WT CI2, and CI2 I20V at pH 4.5, 4 °C were assigned using isotopically-enriched protein expressed in minimal media containing ^{13}C D-glucose and ^{15}N NH_4Cl (Cambridge Isotope Labs) as the sole sources of carbon and nitrogen, respectively, and then purified as described above. HNCACB spectra were acquired with 10% sampling in the indirect dimensions using a Poisson gap scheduling scheme (http://gwagner.med.harvard.edu/intranet/hmsIST/gensched_new.html).[9-10]

Spectra were processed using NMRpipe and reconstructed with the SMILE algorithm.[11] Backbone resonances for WT GB1 and I20V CI2 at pH 7.5, 22 °C were assigned in the same manner. Other assignments (WT CI2 at pH 7.5 and 22 °C, I6L GB1 under both conditions) were transferred. Assignments and labeled spectra are provided in Tables S1-S4 and Figures S1-S4, respectively.

Solution hydrogen-deuterium exchange

Lyophilized aliquots of purified, ^{15}N-enriched protein were resuspended in 650 µL of 7.5-mM HEPES, pH 6.5, flash frozen and lyophilized. After ~24 h, the samples were removed, resuspended in 650 µL 99% D_2O and immediately used to acquire serial NMR HSQC spectra at 22 °C. To capture decay curves for residues that completely exchange in 2 - 24 h (intermediate regime), 10 - 12 sensitivity ^{15}N-^{1}H HSQC spectra were acquired serially over ~12 h. For slowly exchanging residues (>24 h), samples were resuspended, and following acquisition of the first spectrum (0 h timepoint), placed in an incubator at 22 °C. Samples were removed from the incubator every 1 - 3 days for spectrum acquisition.

The rate analysis tool in NMRViewJ was used to fit peak volumes as a function of time to the 3-parameter equation $V = Ae^{-Bt}$, where V is peak volume in arbitrary units, A is a scaling factor, t is time in s, and B is the observed rate constant (k_{obs}). For each residue, k_{obs} was divided by the estimated intrinsic rate constant of exchange (k_{int}) at pH 7.5, 22 °C to approximate the opening equilibrium constant, K_{op}. Values of k_{int} were obtained using the online Server Program for Hydrogen Exchange Rate Estimation, SPHERE.[12] To ensure accurate k_{obs} values, only crosspeak volumes that decayed to

~30% of their initial value were analyzed. Opening free energies, $\Delta G^{\circ\prime}_{op}$ values, were calculated using the equation

$$\mathbf{\Delta G_{op}}^{\circ\prime} = -RTln(K_{op}) = -RTln(\frac{k_{obs}}{k_{int}})$$

where *R* is the gas constant and *T* is the absolute temperature.[13-14]

Liquid Observed Vapor Exchange (LOVE) NMR

For each experiment, two identical aliquots of pure, lyophilized, ^{15}N-enriched protein were resuspended in 650 *μ*L of 1.5-mM HEPES, pH 6.5, to a final protein concentration of 500 *μ*M, flash-frozen, and lyophilized (LABCONCO FreeZone 1 Liter Benchtop Freeze Dry System) for 24 h. Following lyophilization, one sample, designated T_0, was immediately resuspended in 650 µL of cold quench buffer (100 mM citrate buffer, pH 4.5, 90% H_2O/10% D_2O) and transferred to an NMR spectrometer for spectrum acquisition at 4°C. The second sample, designated T_{24}, was placed, with the cap open, in a chamber with a controlled relative humidity of ~75%, prepared as described.[2] After 24 h, the T_{24} sample was resuspended in 650 µL of cold quench buffer and an HSQC spectrum obtained with the same acquisition parameters used for the T_0 sample.

To enable back-exchange correction, the T_{24} sample was left in the spectrometer at 4°C for ~ 12 h, during which time an additional 10-12 spectra were acquired. The time between resuspension and initiation of the first T_{24} spectrum acquisition was 10 min, ~8 min of which were spent at 4 °C.

Identifying residues that back-exchange completely before spectrum acquisition

To differentiate residues that are highly protected from back-exchange from those that back-exchange completely before the first T_{24} spectrum was acquired, a sample of ^{15}N-enriched protein was resuspended to 500 µM in 1.5 mM HEPES, lyophilized for 24 h, resuspended in cold D_2O-based quench buffer (100 mM citrate, pH 4.5 >98% D_2O) and immediately transferred to a spectrometer at 4°C for acquisition of a ^{15}N-^{1}H HSQC spectrum using the same acquisition parameters used for the T_0 and T_{24} samples. Resonances present in H_2O but not in D_2O are presumed to back-exchange completely before the first T_{24} spectrum is acquired. Given that an exchange rate cannot be estimated for these residues, we cannot approximate the pre-back-exchange signal, and, therefore, these residues are omitted from the dataset (see figure captions for lists). We call these resonances “quench labeled”.

Estimating V_{T24}, the peak volume of T_{24} sample pre-back-exchange

For non-quench-labeled T_{24} resonances that exhibited a ≤5% increase in peak volume over ~12 h, back-exchange during the time it takes to acquire a HSQC spectrum (20 min here) is presumed to be negligible. Therefore, for these residues, $\mathbf{V_{T24}}$ is equivalent to the peak volume obtained from integrating the initial T_{24} spectrum.

For T_{24} resonances that exhibited a >5% increase in peak volume over ~12 h, peak volumes from the 10 - 12 spectra acquired serially for the T_{24} sample were plotted as a function of time and fit, using the nonlinear least-squares algorithm in MATLAB, to the 3-parameter equation $V(t) = A(1-e^{-Bt}) + C$, where t is the time between protein resuspension and signal acquisition, V(t) is the peak volume at time t, A is the maximum possible

change in peak volume, B is the observed rate constant, and C is a constant equivalent to the initial peak volume before back-exchange. For these residues, the fitted value for C was used to estimate the pre-back-exchange peak volume, V_{T24}.

The estimated deadtime was 20 min (based on the 10 min between resuspension and initiation of spectrum acquisition plus 10 min for spectrum acquisition). In practice, this estimation means timepoints are shifted by 20 min, e.g. the first spectrum acquired for T_{24} corresponds to the 20-minute timepoint.

Calculating average %Protected from vapor exchange

To determine the average percent of the dried protein population for which a given amide proton is protected from vapor exchange, the average value of V_{T24} (obtained as described above) was divided by the average peak volume of the corresponding crosspeak in the non-vapor-exchanged protein sample (T_0) and multiplied by 100%, i.e. $\overline{\%\boldsymbol{Protected}} = \mathbf{100}\%\, \boldsymbol{x} \frac{\overline{V_{T24}}}{\overline{V_{T0}}}$. Uncertainties were obtained using triplicate analysis and standard propagation of error.

Fourier transform infrared (FTIR) spectroscopy

ATR-FTIR spectra were recorded on a BioTools Prota-3S spectrophotometer equipped with a HgCdTe detector and a ZnSe-diamond attenuated total-internal-reflectance crystal. Spectra comprise 400 scans and were acquired from 805 to 5500 cm^{-1} at 4 cm^{-1} resolution with dry-air purging. Background, buffer, and vapor spectra were acquired at 30 ^{o}C using a Pike Peltier temperature controller.

Empty, path-, buffer-, and sample- spectra were acquired and preprocessed for each sample using Prota3s (BioTools) software. The background spectrum was subtracted from both the buffer- and sample- spectra to produce theabsorbance spectra. The buffer absorbance spectrum (7.5 mM HEPES at 30 ^{o}C) was then subtracted from the sample absorbance spectrum in the same proportion for all samples. To ensure full buffer subtraction, the procedure was performed such that the region at 3750 cm^{-1} is non-negative and the region from 2000 cm^{-1} to 1800 cm^{-1} is flat.

Spectra were processed using an Orange Datamining workflow,[15] and smoothed using 4-component principle-component-analysis denoising.[16] Smoothed bands were processed using a positive rubber band baseline-correction, vector-normalization, and then fit to Voigt profiles through a non-linear least-squares regression.[17] Peaks were assigned and their areas normalized against the total peak area to obtain the percentage of each type of resonance (Table S1); percent secondary structure was calculated from the total peak area excluding the contribution from aromatics. Second derivative spectra were calculated using a Savitzky-Golay filter with a window size of nine points and a second-order polynomial.[18]

Supplementary figures

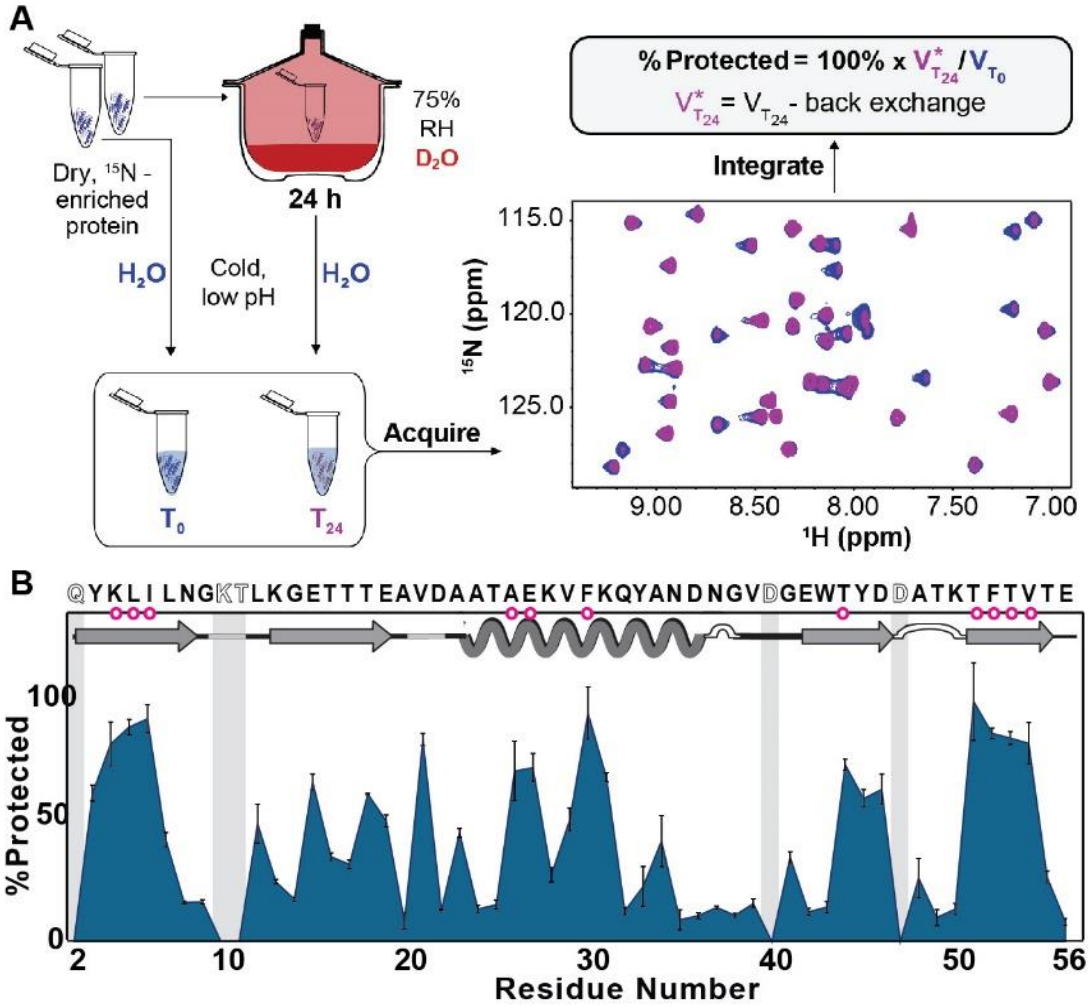

Figure S1. Adjusted LOVE NMR workflow and output. (A) LOVE NMR workflow. Identical samples of ^{15}N-enriched protein dried alone or in the presence of a cosolute are resuspended in cold, acidic buffer before (T_0) or after (T_{24}) 24 h exposure to D_2O vapor at 75% relative humidity (RH). Amide protons unprotected in the dry state exchange with deuterons from the vapor, resulting in smaller cross peak volumes in the T_{24} ^{15}N-^{1}H HSQC spectrum relative to the T_0 spectrum (pink and blue cross peaks, respectively). To correct for solution back-exchange that occurs before and during spectrum acquisition, serial HSQC spectra are obtained for the T_{24} sample, integrated, and fit to the equation $V_{T24}(t) = A(1\text{-}e^{-bt})+V_{T24}*$, where $V_{T24}$is peak volume, t is time since resuspension, A is a scaling factor, b is the observed rate of exchange, and $V_{T24}*$ the peak volume before any back exchange (see Materials and Methods). The fitted $V_{T24}*$ value is then divided by the maximum possible peak volume, V_{T0}, and multiplied by 100 to obtain %Protected. **(B)** LOVE profile of model protein GB1 freeze-dried in 1.5 mM HEPES, pH 6.5. Open letters indicate residues with undefined dry-state protection because they are 100% quench-labelled. Secondary structure (arrows, β-strands; undulations, helix; white bumps, turns; gray lines, bends) is shown at top, with magenta circles indicating solution global unfolding residues. Gray areas indication the absence of data. Error bars represent uncertainty propagated from standard deviations of the mean from triplicate analysis.

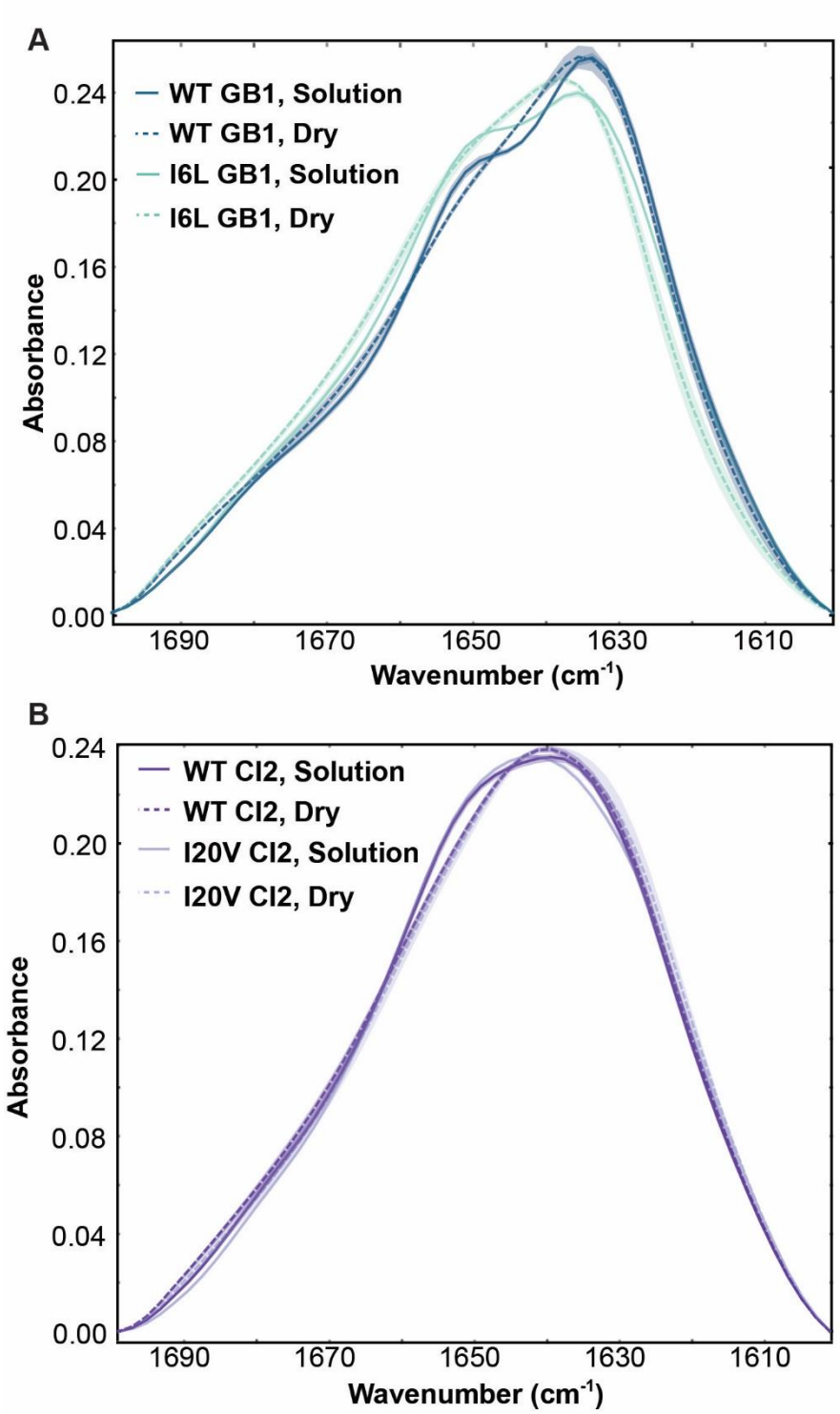

Figure S2. Average ATR-FTIR spectra of GB1 and CI2 variants. Amide-I regions of the averaged spectra of **(A)** GB1 variants and **(B)** CI2 variants in the solution and dry states. Averages are from triplicate analysis. Shaded areas represent the range.

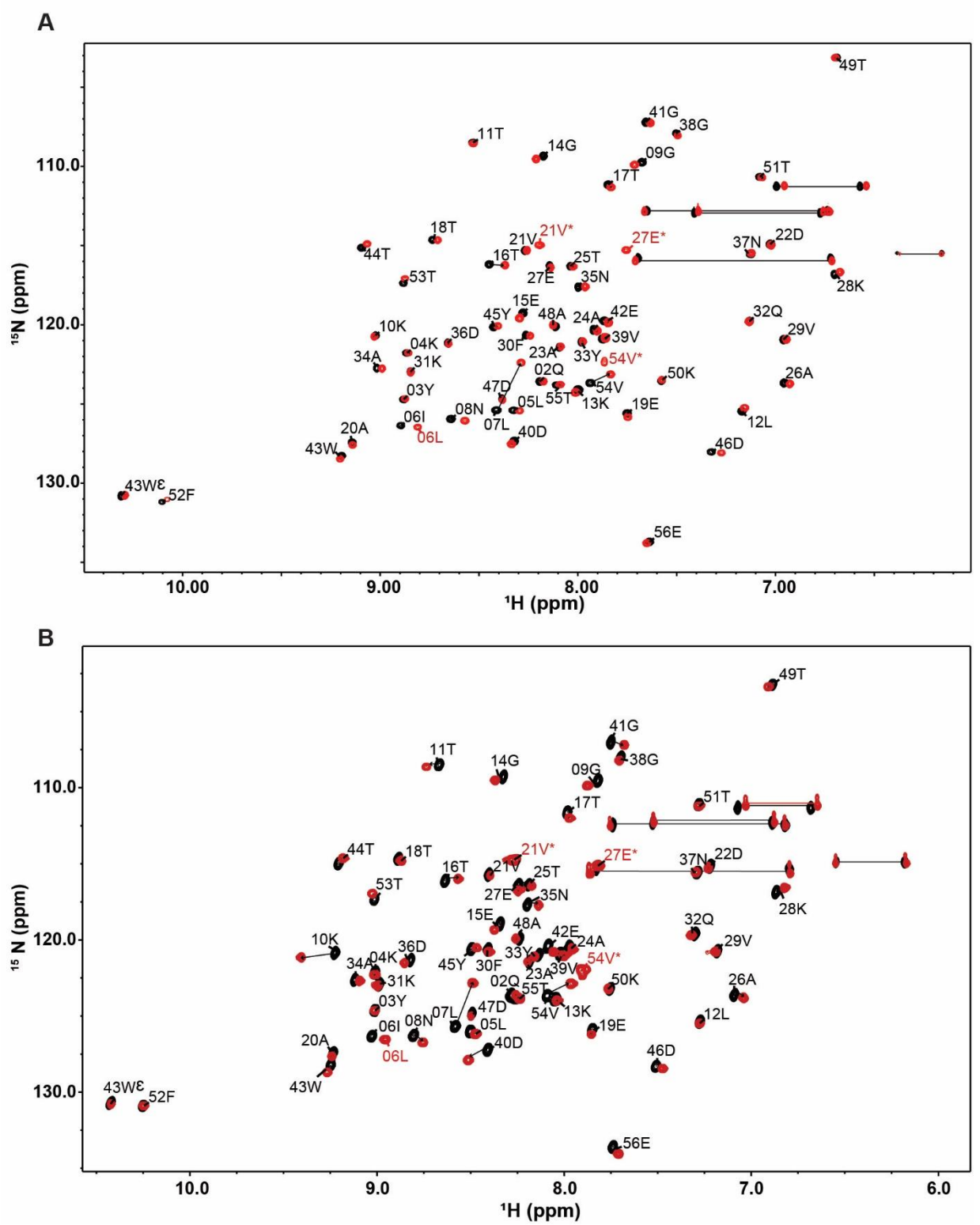

Figure S3. Assigned ^{1}H-^{15}N HSQC spectra of GB1 variants. A) Under spectrum acquisition conditions used for LOVE NMR experiments (100 mM citrate in 90%H_2O, 10% D_2O, pH 4.5, 4°C). B) Under conditions similar to those used for solution hydrogen-deuterium exchange (7.5 mM HEPES in 95%H_2O, 5% D_2O, pH 7.5, 22°C. WT GB1 resonances shown in black, I6L in red. *Starred resonances arise from an alternative conformation.

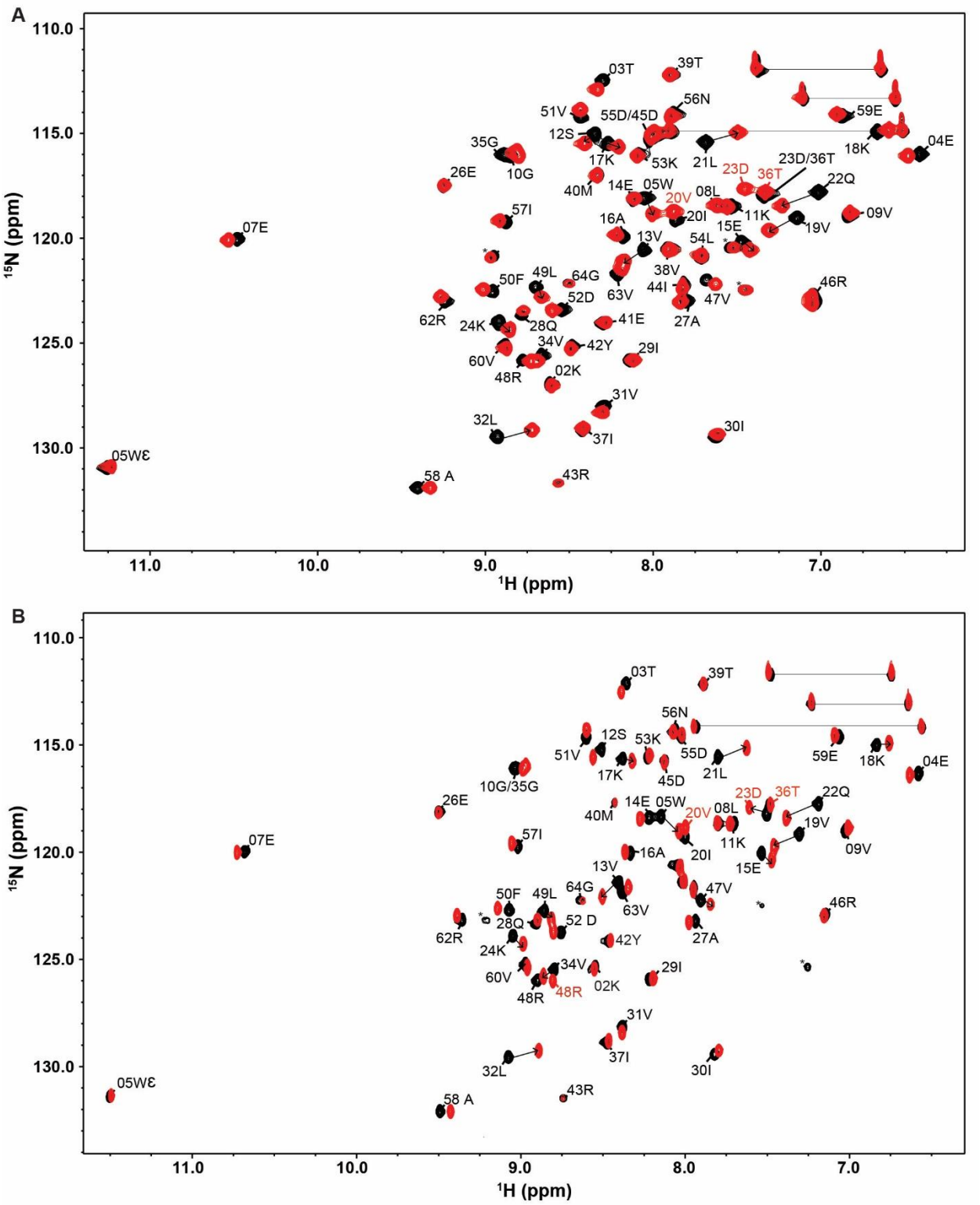

Figure S4. Assigned ^{1}H-^{15}N HSQC spectra of CI2 variants. A) Under spectrum acquisition conditions used for LOVE NMR experiments (100 mM citrate in 90%H_2O, 10% D_2O, pH 4.5, 4°C). B) Under conditions similar to those used for solution hydrogen-deuterium exchange (7.5 mM HEPES in 95%H_2O, 5% D_2O, pH 7.5, 22°C. WT CI2 resonances shown in black, I20V in red. *Starred resonances arise from an alternate conformation.

Supplementary tables

Table S1. FTIR peak locations and secondary structure assignments.

GB1 variants in solution						
	Aromatics	**β-sheet**	**β-sheet**	**α-helix**	**Turn**	**β-sheet**
WT	1617.2 ±0.3 cm^{-1} 4.9 ± 0.2%	1626.9 ±0.2 cm^{-1} 29.1 ± 0.3%	1635.6 ±0.2 cm^{-1} 17.2 ± 0.4%	1650.0 ±0.1 cm^{-1} 35.6 ± 0.5%	1665.2 ±0.1 cm^{-1} 12.2 ± 0.3%	1678.8 ±0.1 cm^{-1} 5.9 ± 0.2%
I6L	1617.0 ±0.2 cm^{-1} 4.9 ± 0.2%	1626.9 ±0.3 cm^{-1} 27.4 ± 0.2%	1636.2 ±0.1 cm^{-1} 16.1 ± 0.4%	1649.9 ±0.1 cm^{-1} 34.6%	1663.9 ±0.3 cm^{-1} 15.1%	1677.9 ±0.2 cm^{-1} 6.8%
GB1 variants, lyophilized						
	Aromatics	**β-sheet**	**β-sheet**	**α-helix**	**Turn**	**Aromatics**
WT	1619.0 ±0.8 cm^{-1} 6.2 ± 0.2%	1628.9 ±0.7 cm^{-1} 26.6 ± 0.1%	1637.8 ±0.5 cm^{-1} 22 ± 1%	1650.0 ±0.6 cm^{-1} 28.9 ± 0.3%	1664.5 ±0.7 cm^{-1} 16.3 ± 0.8%	1619.0 ±0.8 cm^{-1} 6.4 ± 0.4%
I6L	1621 ±1 cm^{-1} 6.3 ± 0.3%	1631 ±1 cm^{-1} 26.1 ± 0.1%	1640 ±1 cm^{-1} 22 ± 1%	1652 ±1 cm^{-1} 28.9 ± 0.3%	1666±1 cm^{-1} 16.4 ± 0.6%	1621 ±1 cm^{-1} 6.2 ± 0.4%
CI2 variants in solution						
	Aromatics	**β-sheet**	**Random Coil**	**α-helix**	**Turn**	**β-sheet**
WT	1617.1 ±0.2 cm^{-1} 5.4 ± 0.1%	1627.1 ±0.2 cm^{-1} 17.6 ± 0.3%	1637.3 ±0.2 cm^{-1} 27.2 ± 0.1%	1649.5 ±0.2 cm^{-1} 30.2 ± 0.4%	1661.8 ±0.3 cm^{-1} 17.8 ± 0.3%	1676.4 ±0.3 cm^{-1} 7.2 ± 0.1%
I20V	1616.7 ±0.2 cm^{-1} 5.7 ± 0.1%	1626.8 ±0.2 cm^{-1} 18.3 ± 0.3%	1637.5±0.1 cm^{-1} 27.1 ± 0.3%	1649.1 ±0.2 cm^{-1} 29.0 ± 0.4%	1660.9 ±0.3 cm^{-1} 18.7 ± 0.3%	1675.3 ±0.3 cm^{-1} 7.0 ± 0.1%
CI2 variants, lyophilized						
	Aromatics	**β-sheet**	**Random Coil**	**α-helix**	**Turn**	**β-sheet**
WT	1617.5 ±0.2 6.1 ± 0.1%	1627.7 ±0.3 19.1 ± 0.3%	1637.9 ±0.4 26.5 ± 0.6%	1649.0 ±0.5 27.1 ± 0.4%	1661.9 ±0.5 19.7 ± 0.4%	1677.0 ±0.3 7.6 ± 0.2%
I20V	1616.7 ±0.2 5.8 ± 0.2%	1626.8 ±0.2 17.6 ± 0.5%	1637.5 ±0.1 24 ± 1%	1649.1 ±0.2 27.8 ± 0.4%	1660.9 ±0.3 22 ± 1%	1675.3 ±0.3 8.3 ± 0.3%

Assignments made using literature values[17-19] and PDB files 2CI2 and 2QMT. Fits returned χ^2 values of ~2 x 10^{-5}.

Table S2. Opening free energies of WT and I6L GB1 at pH 7.5, 22°C.

Residue[§]	$\Delta G_{op}°'$ ± STD[‡] (kcal/mol) WT GB1			I6L GB1		
03Y	7.59	±	0.01	7.09	±	0.01
04K	8.19	±	0.01	7.3	±	0.1
05L	8.126	±	0.004	7.3	±	0.02
06I/L	8.11	±	0.02	7.07	±	0.02
07L	6.16	±	0.04	6.68	±	0.02
18T	7.00	±	0.04	6.69	±	0.02
26A	8.62	±	0.01	8.06	±	0.02
27E	8.43	±	0.01	7.5	±	0.1
28K	5.89	±	0.03	6.02	±	0.01
29V	5.84	±	0.03	5.99	±	0.02
30F	8.53	±	0.01	7.78	±	0.03
31K	8.648	±	0.004	7.87	±	0.01
32Q	5.55	±	0.04	5.76	±	0.03
33Y	6.61	±	0.04	6.64	±	0.01
34A	7.36	±	0.02	7.3	±	0.1
35N	6.97	±	0.04	6.80	±	0.05
36D	5.60	±	0.04	5.61	±	0.06
37N	6.30	±	0.03	6.26	±	0.02
39V	6.11	±	0.03	6.07	±	0.01
42E	5.45	±	0.04	5.50	±	0.04
44T	8.755	±	0.003	8.03	±	0.02
46D	7.60	±	0.01	7.50	±	0.01
50K	5.70	±	0.03	5.90	±	0.02
51T	8.64	±	0.01	7.87	±	0.02
52F	8.64	±	0.01	7.78	±	0.01
53T	8.606	±	0.005	7.72	±	0.03
54V	8.333	±	0.004	7.57	±	0.02
55T	6.83	±	0.04	6.62	±	0.02
56E	2.90	±	0.03	2.73	±	0.03

Footnotes

[§] $\Delta G_{op}°'$ values for residues that exchange slowly enough to be measured.

[‡] Sample standard deviation calculated from three independent experiments.

Table S3. Opening free energies of WT and I20V Cl2 at pH 7.5, 22°C.

Residue[§]	ΔG_{op}°′ ±STD[‡] (kcal/mol) WT Cl2			I20V Cl2		
05W	7.2	±	0.1	7.32	±	0.05
08L	6.6	±	0.1	6.80	±	0.04
09V	5.7	±	0.1	5.93	±	0.02
11K	9.114	±	0.004	9.515	±	0.003
13V	5.8	±	0.1	6.56	±	0.02
16A	7.6	±	0.1	8.0	±	0.1
17K	5.2	±	0.1	5.83	±	0.02
18K	6.1	±	0.1	6.91	±	0.02
19V	7.0	±	0.1	7.74	±	0.07
20I	9.69	±	0.01	9.526	±	0.002
21L	8.01	±	0.01	8.945	±	0.005
22Q	7.4	±	0.1	8.17	±	0.07
24K	7.6	±	0.1	7.90	±	0.06
27A	5.9	±	0.1	6.33	±	0.02
28Q	6.2	±	0.1	7.01	±	0.06
30I	7.782	±	0.002	8.142	±	0.005
32L	7.798	±	0.004	8.672	±	0.004
35G	5.7	±	0.1	6.21	±	0.02
46R	7.7	±	0.1	7.91	±	0.05
47V	9.61	±	0.02	9.76	±	0.01
48R	8.0	±	0.1	8.28	±	0.07
49L	10.592	±	0.009	9.901	±	0.008
50F	9.166	±	0.008	9.350	±	0.003
51V	9.37	±	0.01	9.810	±	0.003
52D	6.8	±	0.1	7.41	±	0.05
56N	8.1	±	0.1	8.71	±	0.06
57I	7.89	±	0.01	8.88	±	0.008
58A	6.6	±	0.1	7.06	±	0.02
59E	7.2	±	0.1	7.55	±	0.06
62R	8.31	±	0.01	8.523	±	0.006
63Y	6.7	±	0.1	7.02	±	0.04
64G	6.40	±	0.01	6.785	±	0.006

Footnotes

[§] ΔG_{op}°′ values from for non-proline residues without overlapping peaks that exchange slowly enough to be measured.

[‡] Sample standard deviation calculated from three independent experiments.

Table S4. Average %Protected values of WT and I6L GB1 freeze-dried in 1.5 mM HEPES pH 6.5.

Residue	%Protected ±STD‡ WT GB1			I6L GB1		
3	61	±	3	57	±	7
4	81	±	9	72	±	3
5	88	±	3	95	±	7
6	92	±	6	91	±	5
7	42	±	3	47	±	3
8	16	±	1	23	±	1
9	16	±	1	24	±	6
12	49	±	8	54	±	1
13	25	±	1	34	±	8
14	17	±	1	33	±	2
15	66	±	3	62	±	5
16	35	±	2	42	±	1
17	32	±	2	40	±	20
18	60.7	±	0.4	51	±	5
19	50	±	2	60	±	30
20	8	±	3	11	±	1
22	13.1	±	0.3	12	±	3
23	45	±	2	60	±	20
24	13	±	1	15	±	5
25	15	±	2	12	±	3
26	70	±	10	74	±	2
27	72	±	6	100	±	30
28	28	±	3	32	±	7
29	50	±	5	59	±	6
30	90	±	10	99	±	10
31	68	±	2	64	±	5
32	13	±	1	15	±	3
33	23	±	8	29	±	6
34	41	±	10	34	±	6
35	9	±	4	14	±	2
36	11	±	1	13	±	1
37	14	±	1	14	±	0
38	11	±	1	16	±	5
39	16	±	2	12	±	4
41	35	±	2	43	±	13
42	12	±	1	9	±	4
43	14	±	2	20	±	10
44	73	±	2	60	±	4
45	59	±	4	80	±	30
46	63	±	6	60	±	10
48	26	±	8	50	±	20
49	10	±	3	8	±	6
50	13	±	2	30	±	40
51	100	±	20	84	±	3
52	86	±	2	100	±	20
53	84	±	3	80	±	2
54	81	±	9	70	±	30
55	27	±	2	25	±	7
56	8	±	1	8	±	3

Table S5. Average %Protected values of WT and I20V CI2 freeze-dried in 1.5 mM HEPES pH 6.5.

Residue	%Protected ±STD‡ WT CI2			I20V CI2		
4	10	±	10	10	±	4
5	51	±	3	15	±	7
7	33	±	4	40	±	20
8	100	±	20	40	±	10
9	50	±	20	13	±	2
11	73	±	8	70	±	10
12	11	±	3	15	±	7
13	20	±	20	8	±	4
14	17	±	3	38	±	2
15	15	±	1	10	±	10
16	100	±	8	64	±	8
17	20	±	7	9	±	3
18	30	±	20	13	±	1
19	111	±	8	70	±	7
20	100	±	20	90	±	20
21	84	±	7	80	±	10
22	60	±	8	50	±	10
24	70	±	5	55	±	7
26	21	±	3	30	±	20
27	16	±	9	0	±	10
28	4	±	6	0	±	10
29	10	±	5	10	±	3
30	80	±	8	86	±	6
31	70	±	6	60	±	8
32	90	±	10	90	±	20
37	22	±	3	30	±	20
38	14	±	8	14	±	6
39	60	±	10	61	±	8
42	35	±	4	50	±	7
43	0	±	5	0	±	10
44	10	±	20	10	±	20
46	83	±	9	80	±	10
47	80	±	20	80	±	10
49	100	±	10	97	±	5
50	85	±	9	70	±	6
51	84	±	6	74	±	5
52	70	±	20	70	±	4
54	46	±	2	50	±	10
56	90	±	10	88	±	5
57	82	±	6	82	±	7
58	80	±	10	78	±	3
59	80	±	20	80	±	2
60	70	±	10	90	±	6
62	60	±	10	20	±	10
63	40	±	10	13	±	3
64	60	±	30	50	±	10

References

1. Glasoe, P. K.; Long, F. A., Use of Glass Electrodes to Measure Acidities in Deuterium Oxide. *J. Phys. Chem.* **1960,** *64* (1), 188-190.
2. Crilly, C. J.; Brom, J. A.; Kowalewski, M. E.; Piszkiewicz, S.; Pielak, G. J., Dried Protein Structure Revealed at the Residue Level by Liquid-Observed Vapor Exchange NMR. *Biochemistry* **2021,** *60* (2), 152-159.
3. Monteith, W. B.; Pielak, G. J., Residue Level Quantification of Protein Stability in Living Cells. *Proc. Natl. Acad. Sci. USA* **2014,** *111* (31), 11335-11340.
4. Smith, C. K.; Withka, J. M.; Regan, L., A Thermodynamic Scale for Theβ-Sheet Forming Tendencies of the Amino Acids. *Biochemistry* **1994,** *33* (18), 5510-5517.
5. Charlton, L. M.; Barnes, C. O.; Li, C.; Orans, J.; Young, G. B.; Pielak, G. J., Residue-Level Interrogation of Macromolecular Crowding Effects on Protein Stability. *J. Am. Chem. Soc.* **2008,** *130* (21), 6826-6830.
6. Gill, S. C.; von Hippel, P. H., Calculation of Protein Extinction Coefficients from Amino Acid Sequence Data. *Anal. Biochem.* **1989,** *182* (2), 319-326.
7. Delaglio, F.; Grzesiek, S.; Vuister, G. W.; Zhu, G.; Pfeifer, J.; Bax, A., NMRPipe: A Multidimensional Spectral Processing System Based on Unix Pipes. *J. Biomol. NMR* **1995,** *6* (3), 277-293.
8. Johnson, B. A.; Blevins, R. A., NMR View: A Computer Program for the Visualization and Analysis of NMR Data. *J. Biomol. NMR* **1994,** *4* (5), 603-614.
9. Miljenović, T. M.; Jia, X.; Mobli, M., Nonuniform Sampling in Biomolecular NMR. In *Modern Magnetic Resonance*, 2nd ed.; Webb, G. A., Ed. Springer International Publishing: Cham, 2017; pp 1-21.
10. Hyberts, S. G.; Takeuchi, K.; Wagner, G., Poisson-Gap Sampling and Forward Maximum Entropy Reconstruction for Enhancing the Resolution and Sensitivity of Protein NMR Data. *J. Am. Chem. Soc.* **2010,** *132* (7), 2145-2147.
11. Ying, J.; Delaglio, F.; Torchia, D. A.; Bax, A., Sparse Multidimensional Iterative Lineshape-Enhanced (Smile) Reconstruction of Both Non-Uniformly Sampled and Conventional NMR Data. *J. Biomol. NMR* **2017,** *68* (2), 101-118.
12. Zhang, Y.-Z. Protein and Peptide Structure and Interactions Studied by Hydrogen Exchange and NMR. PhD thesis, University of Pennsylvania, Philadelphia, 1995.
13. Englander, S. W.; Kallenbach, N. R., Hydrogen Exchange and Structural Dynamics of Proteins and Nucleic Acids. *Q. Rev. Biophys.* **1983,** *16* (4), 521-655.
14. Miklos, A. C.; Li, C.; Pielak, G. J., Using NMR-Detected Backbone Amide ^{1}H Exchange to Assess Macromolecular Crowding Effects on Globular-Protein Stability. *Methods Enzymol.* **2009,** *466*, 1-18.
15. Demšar, J.; Curk, T.; Erjavec, A.; Gorup, Č.; Hočevar, T.; Milutinovič, M.; Možina, M.; Polajnar, M.; Toplak, M.; Starič, A., Orange: Data Mining Toolbox in Python. *Journal of Machine Learning Research* **2013,** *14* (1), 2349-2353.
16. Koziol, P.; Raczkowska, M. K.; Skibinska, J.; Urbaniak-Wasik, S.; Paluszkiewicz, C.; Kwiatek, W.; Wrobel, T. P., Comparison of Spectral and Spatial Denoising Techniques in the Context of High Definition FT-Ir Imaging Hyperspectral Data. *Sci. Rep.* **2018,** *8* (1), 14351.
17. Sadat, A.; Joye, I. J., Peak Fitting Applied to Fourier Transform Infrared and Raman Spectroscopic Analysis of Proteins. *Appl. Sci.* **2020,** *10* (17).
18. Gautam, R.; Vanga, S.; Ariese, F.; Umapathy, S., Review of Multidimensional Data Processing Approaches for Raman and Infrared Spectroscopy. *EPJ Techniques and Instrumentation* **2015,** *2* (1), 8.
19. Martinez, G.; Millhauser, G., FTIR Spectroscopy of Alanine-Based Peptides: Assignment of the Amide I′ Modes for Random Coil and Helix. *J. Struct. Biol.* **1995,** *114* (1), 23-27.